

DISCRETE CRACK MODELING IN CONCRETE STRUCTURES

J Červenka and V. E. Saouma,
Dept. of Civil Environmental & Architectural Engineering, University of Colorado,
Boulder, Colorado, U.S.A.

Abstract

A comprehensive and integrated approach to the nonlinear modeling of concrete structures using the discrete crack model in the finite element method is proposed. Three interrelated models are used: (1) solid model of a cracked structure, (2) finite element model and (3) linear and nonlinear fracture mechanics based model. Thus, for each crack increment a solid model is modified and a finite element mesh is automatically regenerated and reanalyzed. Both linear and nonlinear fracture mechanics theories are considered. A new implementation of the domain integral method is proposed for the computation of stress intensity factors along a general three-dimensional crack front. For the nonlinear theory, an interface crack model, which includes shear effects, is used to model the fracture process zone in cementitious materials. The proposed methodology is verified on numerous problems with known experimental or analytical results, and is also applied to both two- and three-dimensional nonlinear analyses of concrete dams.

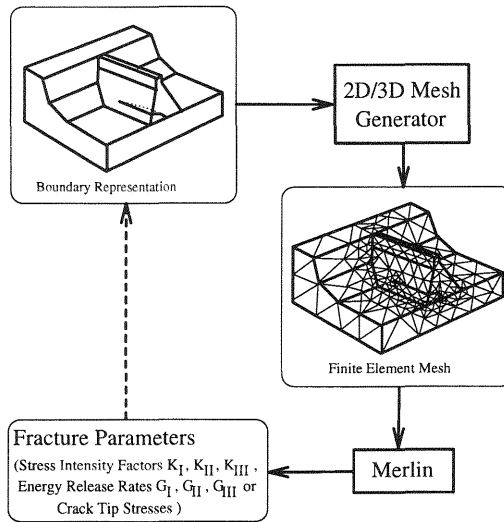


Figure 1: Modeling of crack propagation

1 Introduction

It is generally accepted that the discrete crack approach does not exhibit the strong mesh sensitivity as the “classical” smeared crack models (Bažant 1976, de Borst & Rots 1989). In addition, material properties used by the discrete crack model can be readily determined from well established experimental methods. The only disadvantage of this model is the need to modify the finite element mesh at each crack increment. Whereas, various remeshing techniques have been proposed in the literature to address this problem, they all have been restricted to two-dimensional problems.

In this paper, a fundamentally different approach to the remeshing problem is adopted. The finite element model is used only as a tool to solve the differential equations of elasticity, and a boundary representation (i.e. solid model) is used for problem definition. The cracks are considered to be part of this boundary definition. Thus, each time a violation of the crack propagation criterion is detected in the finite element model, a finite element mesh is adaptively regenerated (Fig. 1). From this approach, the classical partial remeshing can be easily recovered as a special case. In addition, this method can be readily extended to error based adaptivity.

For linear elastic fracture mechanics, the general three-dimensional

form of the domain integral, which includes the effects of body forces, crack surface tractions, temperatures and pore pressures, is derived for the evaluation of stress intensity factors along a three-dimensional crack front. An important characteristic of the proposed implementation is that it does not require a special arrangement of finite elements around the crack front. The domain integral is evaluated over a tubular domain defined independently of the mesh layout. A Gauss integration scheme in cylindrical coordinates is devised to facilitate the numerical integration. The new implementation is validated on three-dimensional problems with known analytical solution.

For non-linear fracture mechanics, a new three-dimensional interface crack model (ICM) is derived. The model is a generalization of the classical Hillerborg's fictitious crack model (FCM), which can be recovered if shear displacements are ignored.

Finally, an application of the proposed models to the safety analysis of concrete dams is presented.

2. Linear elastic fracture mechanics

If the zone of damaged or plastified material at the crack tip (i.e. fracture process zone) is small compare to the crack length and structural size, an extremely fine mesh would be necessary to accurately simulate the energy dissipation in this region. For this case, it is more efficient to use linear elastic fracture mechanics. In this work, a new finite element implementation of domain integral method is proposed to evaluate the fracture parameters (i.e. stress intensity factors) along an arbitrary three-dimensional crack front.

2.1 Domain integral method

This method for the numerical evaluation of stress intensity factors along three-dimensional crack fronts was proposed by Li et. al. (1985), Shih et. al. (1988), and under a different name as equivalent energy domain integral by Nikishkov and Atluri (1987). It is very similar to the virtual crack extension method of de Lorenzi (1985) in the sense that the domain integral of Equation 1 represents an energy released by a virtual crack extension $v_l(s)$.

$$\bar{G} = - \int_{\Omega} (P_{lj}q_l)_{,j} d\Omega + \int_{\Sigma_3 \cup \Sigma_4} P_{lj}m_j q_l d\Sigma \quad (1)$$

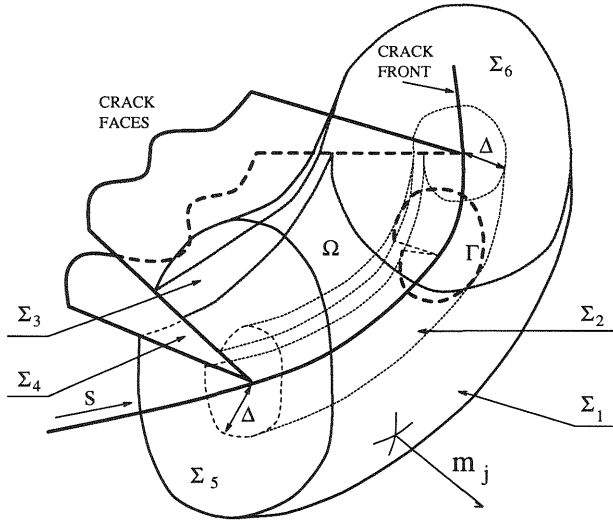


Figure 2: Domain integral derivation

P_{lj} is the Eshelby's energy momentum tensor (Eshelby 1956) and is equal to:

$$P_{ij} = W\delta_{ij} - \sigma_{lj} u_{l,i} \quad (2)$$

where W is the strain energy density, σ_{ij} is the symmetric stress tensor and $u_{l,j}$ are displacement gradients. The domain of integration is shown in Figure 2, where m_j is the surface normal and q_l is a vectorial smoothing function which is equal to $v_l(s)$ along the crack front and zero on the external boundaries of the integration domain Ω . Physically, q_l represents a virtual shift of the elastic fields around the crack front corresponding to a virtual crack extension $v_l(s)$. In order to perform the differentiation of the energy momentum tensor P_{lj} in Equation 1 it is necessary to select constitutive relations for the elastic solid under consideration. In the subsequent derivations, a general elastic solid with body forces, temperatures and internal pore pressures is assumed. The appropriate field equations are substituted into Eq. 1 and the following general three-dimensional form of the domain integral which accounts for the effects of body forces b_i , temperatures τ , pore pressures p and crack surface tractions \hat{t}_i is recovered (Červenka 1994).

$$\bar{G} = \int_{\Omega} (\bar{\sigma}'_{ij} u_{i,l} q_{l,j} - W q_{j,j} + p_{,i} u_{i,l} q_l - b_i u_{i,l} q_l + \alpha_T \mathcal{T}_{,j} \sigma_{ii} q_j) d\Omega$$

$$+ \int_{\Sigma_3 \cup \Sigma_4} (W q_j m_j - \hat{t}_i u_{i,l} q_l - p m_i u_{i,j} q_j) d\Sigma \quad (3)$$

where $\bar{\sigma}'_{ij}$ is the effective stress tensor, $\alpha_{\mathcal{T}}$ is the coefficient of thermal expansion, \mathcal{T} is the temperature difference and \hat{t}_i is the applied surface traction vector along the crack faces. Thus, \bar{G} is a functional in terms of net effective stress field $\bar{\sigma}'_{ij}$, displacement field u_i and weighting function q_l :

$$\bar{G} = \bar{G}(\bar{\sigma}'_{ij}, u_i, q_l) \quad (4)$$

2.2 Finite element implementation

In a finite element implementation of the domain integral, the crack front consists of a finite number of nodes and line segments. Therefore, the pointwise values of energy release rates for co-linear crack propagation G_1 in terms of their nodal counterparts can be defined using crack front shape functions $N_i(s)$:

$$G_1 = \sum_{i=1}^N N_i(s) G_1^i \quad (5)$$

where G_1 is the energy release rate for crack front propagation along direction 1 at point s (i.e. direction perpendicular to the crack front and in the plane of the crack), and G_1^i is the energy release rate for co-linear crack propagation at a crack front node i . In an analogous way, we define a virtual co-linear crack extension corresponding to each crack front node k :

$$v_1^k(s) = \sum_{m=1}^N \Lambda_{1m}^k N_m(s) \quad (6)$$

where N is the number of crack front nodes, and Λ_{1m}^k is a square $N \times N$ matrix of displacements coefficients in all three coordinate directions corresponding to a virtual crack displacement at node k . To each $v_1^k(s)$, a corresponding weighting function q_1^k must be defined.

The nodal values G_1^i can be computed by solving the following system of equations, (Li et. al. 1985, Shih et. al. 1988):

$$\mathbf{g}_1 = (\mathbf{\Lambda}_1 \mathbf{C})^{-1} \bar{\mathbf{g}} \quad (7)$$

where $\bar{\mathbf{g}}$ is the vector of domain integral values \bar{G} associated to each crack front node, \mathbf{C} is a weighting matrix similar to the consistent

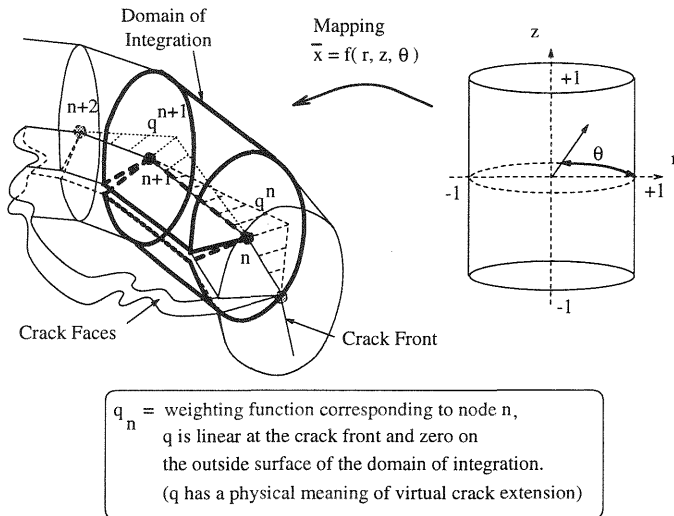


Figure 3: Implementation of domain integral

mass matrix of truss element and \mathbf{g}_1 is the vector of nodal values of energy release rates G_1^i for co-linear crack propagation, which can be subsequently decomposed into the energy release rates for each fracture mode (Nikishkov and Atluri 1987, Červenka 1994)

$$\mathbf{g}_1 = \mathbf{g}_I + \mathbf{g}_{II} + \mathbf{g}_{III} \quad (8)$$

where \mathbf{g}_I , \mathbf{g}_{II} and \mathbf{g}_{III} are vectors of nodal values of energy release rates for the three fracture modes, \mathbf{G}_I , \mathbf{G}_{II} and \mathbf{G}_{III} . For linear elastic fracture mechanics, there exists a direct relationship between G_I , G_{II} , G_{III} and the stress intensity factors K_I , K_{II} , K_{III} , (Nikishkov and Atluri 1987).

The key to solving Equation 7 is the accurate evaluation of the domain integrals \bar{G} for each crack front node (i.e. each virtual crack extension). In the proposed approach, this is accomplished through a numerical integration over cylindrical regions of specified radius around the crack front. Each cylindrical region is then mapped into a unit cylinder, in which the integration is performed using Gauss quadrature (Fig. 3). To the best of the authors knowledge, the Gauss points for circular regions for the integration in polar coordinates have not yet been derived, and the Gauss point coordinates for integration rules up to 40 points are computed and tabulated in

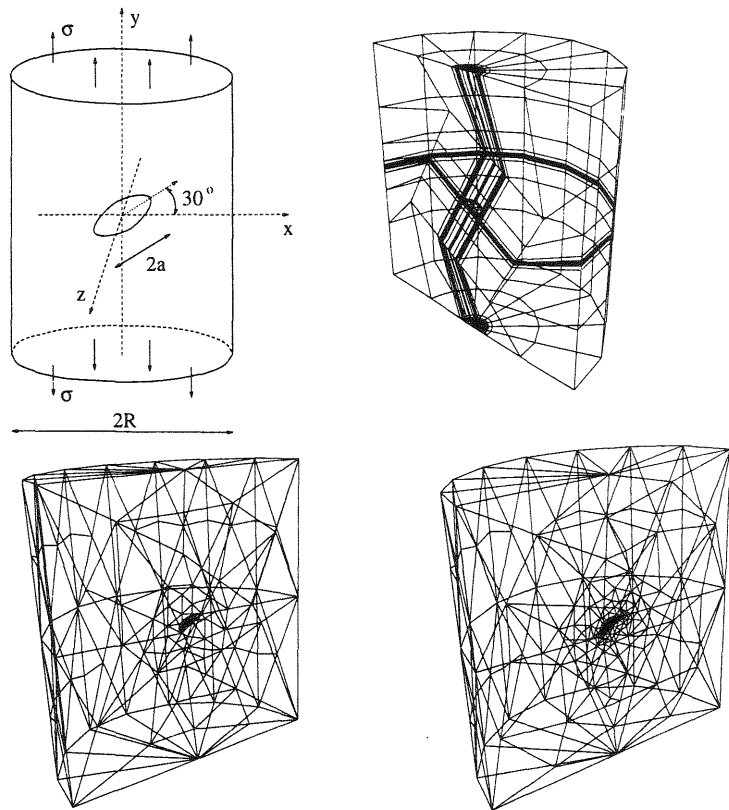


Figure 4: Geometry and meshes for the cylindrical rod with penny shaped crack

Červenka 1994.

2.3 Validation problem

To validate the domain integral implementation in full three-dimensional mixed mode fracture case, an example of a circular inclined crack in a cylindrical rod in tension is analyzed. The analytical solution is taken from Nikishkov and Atluri (1987). The geometry of the problem is shown in Figure 4. Due to the inclination of the interior crack with respect to the direction of applied tractions, the crack front is under a mixed mode fracture condition. All three stress intensity factors are non-zero. The problem is first analyzed using standard isoparametric 8 node brick elements. The finite element mesh is shown in Figure 4 and the distribution of SIF's along the curved

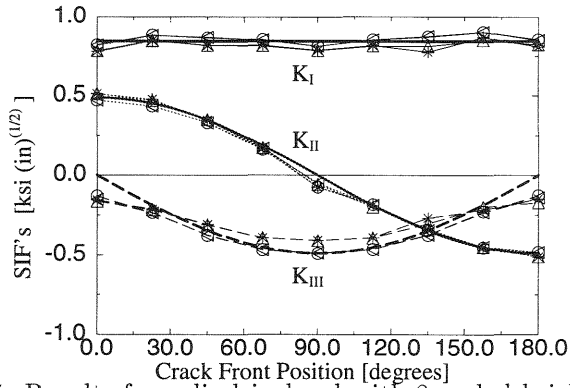


Figure 5: Results for cylindrical rod with 8 noded brick (B8) elements

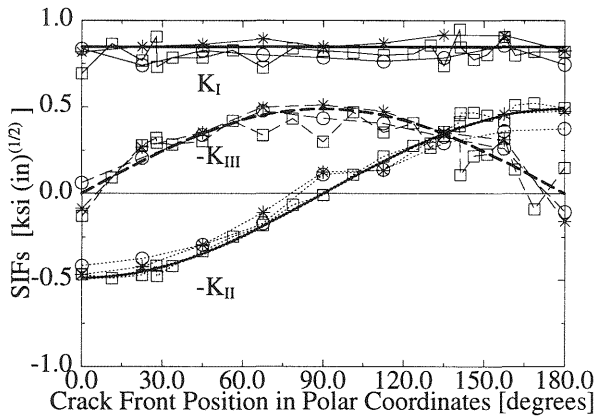


Figure 6: Results for cylindrical rod with tetrahedral (T4, T10) elements

crack front is plotted in Figure 5. The figure shows the comparison with the analytical solution for various radiuses of the integration domain and integration rules. Subsequently, the same problem was analyzed using meshes composed of tetrahedral elements, which were generated automatically (Červenka 1994). Results from this analysis are shown in Figure 6. The problem was analyzed using both T4 and T10 elements (linear and quadratic tetrahedral elements), and different radiuses were used for the evaluation of the domain integral. The results show good agreement with the analytical solution, although they are generally worse than for B8 elements.

In subsequent analysis, the direction of crack propagation was computed based on the maximum circumferential stress criteria (Erdogan and Sih 1963, Červenka 1994). Then, new crack surfaces were inserted into the boundary representation of the structure, and a

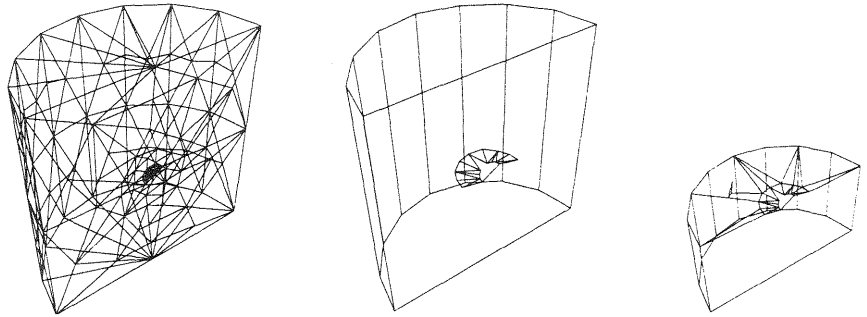


Figure 7: Crack propagation in cylindrical rod, (Reich et. al. 1994, , Červenka 1994)

new mesh was generated and analyzed. This process was repeated until the crack propagated through the whole thickness of the rod, and separated it into two parts. The crack propagation process, shown in Figure 7, demonstrates the application of automatic mesh generation in the three-dimensional mixed mode crack propagation.

3. Non-linear fracture mechanics

It is well known that as the size of concrete structure decreases, one must consider the true nature of cracking, which is not localized into a sharp crack tip, but rather is spread over a certain volume called fracture process zone. Within the framework of discrete crack models, this phenomenon can be simulated by the fictitious crack model of Hillerborg et. al. (1976). In this work, a generalization of this model, which considers shear effects in the fracture process zone, is proposed (Červenka 1994).

3.1 Interface crack model (ICM)

Within the context of the proposed model, a crack is idealized as a line/surface separating the structure, and constitutive relationships between tractions and relative displacements on this surface are derived. The shape of the failure function for the two-dimensional case is shown in Figure 8, and it corresponds to the failure criteria first proposed by Carol et. al. (1992). The general three-dimensional failure function is obtained by mere rotation around the σ -axis. The

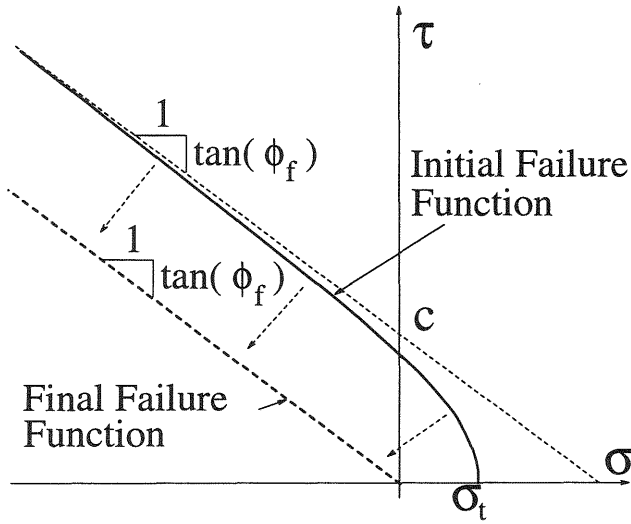


Figure 8: Failure function

evolution of the failure function is based on a softening parameter u^{ieff} which is the norm of the inelastic displacement vector \mathbf{u}^i . The inelastic displacement vector is obtained through decomposition of the displacement vector \mathbf{u} into an elastic part \mathbf{u}^e and an inelastic one \mathbf{u}^i . The inelastic part can subsequently be decomposed into plastic (i.e. irreversible) displacements \mathbf{u}^p and fracturing displacements \mathbf{u}^f . The plastic displacements are assumed to be caused by friction between crack surfaces and the fracturing displacements by the formation of microcracks.

$$\begin{aligned}
 F &= F(c, \sigma_t, \phi_f), \quad c = c(u^{\text{ieff}}), \quad \sigma_t = \sigma_t(u^{\text{ieff}}) \\
 \mathbf{u} &= \mathbf{u}^e + \mathbf{u}^i, \quad \mathbf{u}^i = \mathbf{u}^p + \mathbf{u}^f \\
 u^{\text{ieff}} &= \|\mathbf{u}^i\| = (u_x^i{}^2 + u_y^i{}^2 + u_z^i{}^2)^{1/2}
 \end{aligned} \tag{9}$$

3.2 Non-linear solver

The resulting system of equations is highly non-linear, and if solved by Newton-Raphson method, it would involve non-symmetric and negative stiffness matrices. In this work, a quasi-Newton method based on Davidon rank one update (Davidon 1968) is used, and is supplemented with line search method (Crisfield 1991) to increase robustness for cases with non-symmetric stiffness matrix.

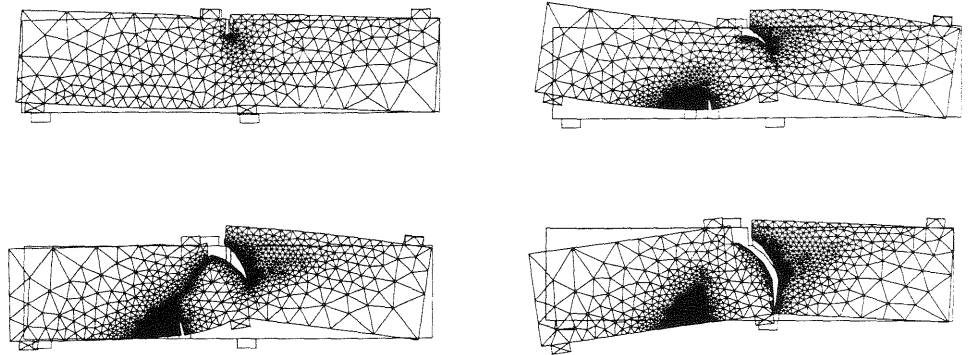


Figure 9: Meshes for crack propagation in shear beam

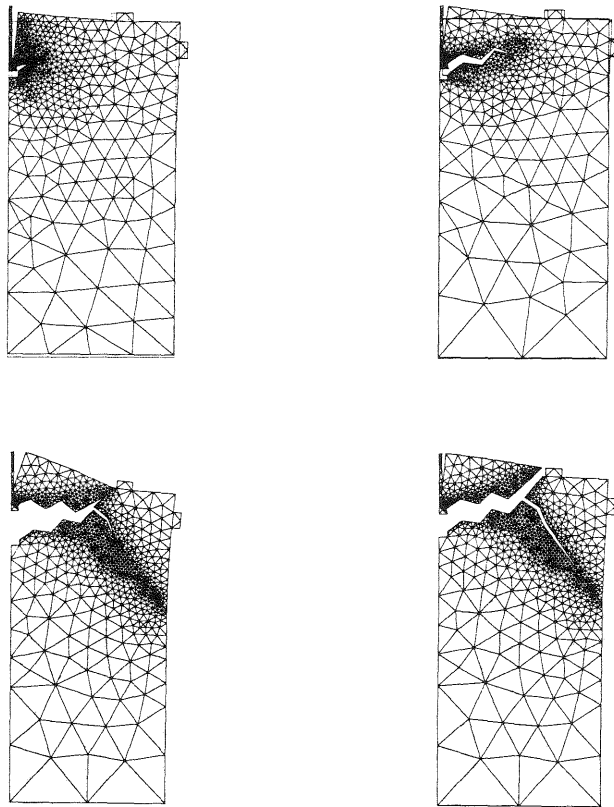


Figure 10: Crack propagation for anchor bolt pull out test I

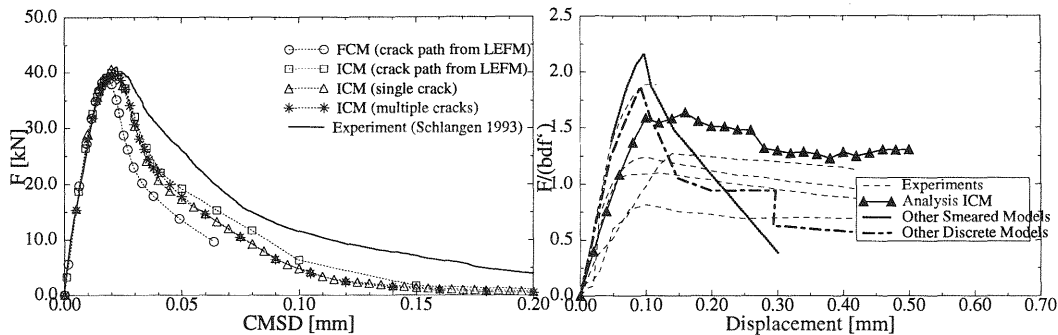


Figure 11: Load-displacement curves for shear beam and anchor pull-out

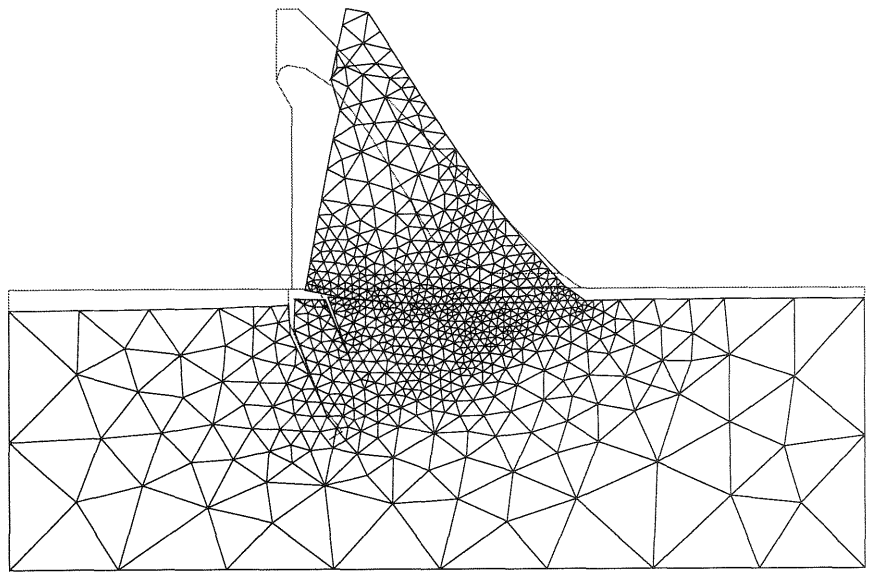
3.3 Validation problems

Large number of problems with known experimental data were analysed to verify and validate the proposed model (Červenka 1994). In this section, two of these examples are presented: first one is a nonlinear analysis of notched concrete beam in shear which was experimentally tested by Schlangen (1993) and second is the anchor bolt pull-out test specified in RILEM and JCI (1993) round robin analysis. The deformed finite element meshes are shown in Figures 9 and 10. The results for the anchor bolt pull-out shown in this paper correspond to the test type I. from JCI (1993). It can be seen that the crack patterns and load-displacement curves (Fig. 11) are in very good agreement with the experimentally observed behaviour.

4. Application to concrete dams

The proposed models were successfully applied to the safety analysis of concrete dams, which was the primary objective of our research. Two examples are presented: a two-dimensional fracture mechanics analysis of a concrete gravity buttressed dam (Fig. 12) and three-dimensional non-linear analysis of an arch dam.

The first analysis was part of the relicensing process of the dam, and both linear and non-linear fracture mechanics were used to estimate the extent of cracking along the interface for subsequent shear friction factor computations. In addition, a full structural response was obtained by combining the non-linear solution methods mentioned in Sec. 3.2 with indirect displacement control methods, and



Regular Plot
Deformed mesh: Scale factor = 1.477e+03

Figure 12: Deformed shape at probable maximal flood load

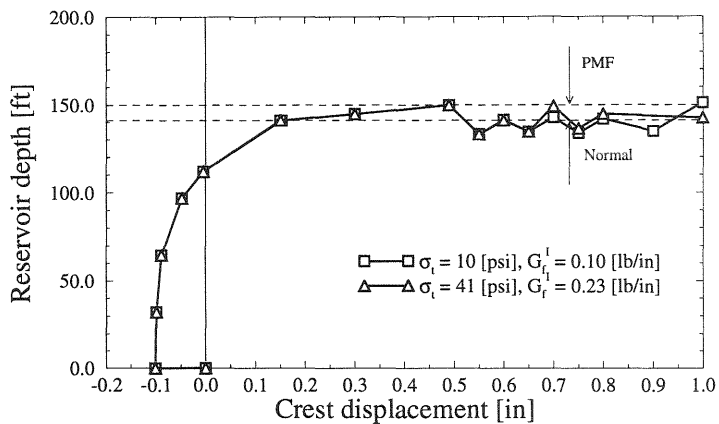


Figure 13: Load-displacement curves for the incremental analysis of a buttressed dam

the results are plotted in terms of water elevation versus crest displacements in Fig. 13.

The second analysis was part of a benchmark round robin study organized by ICOLD (International Committee on Large Dams). The main objective of this analysis was to determine the amount of contraction joint openings in an arch dam during winter and summer loading conditions. Some results from this analysis are in

Fig. 14, which shows the joint openings for winter conditions looking at the dam from downstream. The joint openings in the summer were minimal and the structural response, therefore, remained in the linear region.

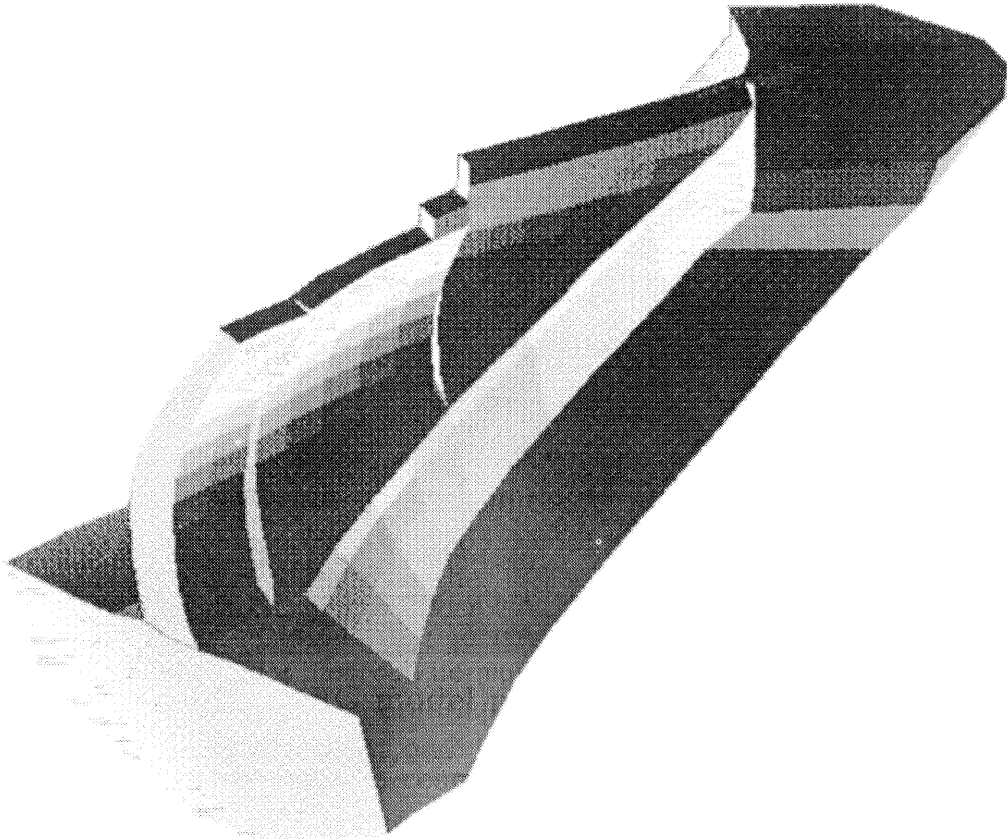


Figure 14: Deformed shape for winter condition, downstream face

Acknowledgements

This research has been funded by the Electric Power Research Institute, Palo-Alto, through Research Contract No. RP-2917-08. The support of its project manager, Mr. Doug Morris, and its project monitor, Mr. Howard Boggs is gratefully acknowledged.

Bibliography

- Bažant, Z.P. (1976) Instability, ductility and size effect in strain softening concrete. **Journal of Engng. Mech.** (ASCE), 102(2),331–344.
- Carol, I., Bažant, Z.P. and Prat, P.C. (1992) Microplane type constitutive models for distributed damage and localized cracking in concrete structures. In **Proc. Fracture Mechanics of Concrete Structures**, pages 299–304, Breckenridge, CO, Elsevier.
- Červenka, J. (1994) **Discrete Crack Modeling in Concrete Structures**. PhD thesis, University of Colorado, Boulder.
- Crisfield, M.A. (1991) **Non-linear Finite Element Analysis of Solids and Structures, Vol 1**. John Willey & Sons.
- Davidon, W.C. (1968) Variance algorithm for minimisation. **Computer J.**, 10,406–410.
- de Borst, R. and Rots, J.G. (1989) Occurrence of spurious mechanisms in computation of strain-softening solids. **Eng. Computations**, 6,272–280.
- deLorenzi, H.G. (1985) Energy release rate calculations by the finite element method. **Engineering Fracture Mechanics**, 21,129–143.
- Erdogan, F. and Sih, G.C. (1963) On the crack extension in plates under plane loading and transverse shear. **Journal of Basic Engineering**, 85,519–527.
- Eshelby, J.D. (1956) The continuum theory of lattice defects. **Solid State Physics**, 3,79–144.
- Hillerborg, A. and Modéer, M. and Petersson, P.E. (1976) Analysis of crack formation and crack growth in concrete by means of fracture mechanics and finite elements. **Cement and Concrete Research**, 6(6),773–782.
- Japanese Concrete Institute (1993) Jci round robin tests and analysis. **Concrete Journal**, 30(2 & 3).
- Li, F. Z. and Shih, C. F. and Needleman, A. (1985) A comparison of methods for calculating energy release rates. **Engineering Fracture Mechanics**, 21(2),405–421.

Nikishkov, G. P. and Atluri, S. N. (1987) Calculation of fracture mechanics parameters for an arbitrary three-dimensional crack, by the 'equivalent domain integral' method. **International Journal of Numerical Methods in Engineering**, 24(9),1801–1821.

Reich, R. and Červenka, J. and Saouma, V. (1994) Merlin: A computational environment for 2d/3d discrete fracture analysis. In H. Mang, N. Bicanic, and de Borst R., editors, **Computational Modelling of Concrete Structures**, pages 999–1008. Pineridge Press, Swansea, UK.

Schlangen, E. (1993) **Experimental and Numerical Analysis of Fracture Processes in Concrete**. PhD thesis, Delft University of Technology.

Shih, C. F. and Moran, B. and Nakamura, T. (1988) Crack tip integrals and domain integral representation for three-dimensional crack problems. In **Analytical, Numerical and Experimental Aspects of Three Dimensional Fracture Processes**, New York, N.Y. (American Society of Mechanical Engineering) AMD 91.